

The formation of antitaxial calcite veins with well-developed fibres, Oppaminda Creek, South Australia

Paul D. Bons*, Michael Montenari

Mineralogie und Geodynamik, Institut für Geowissenschaften, Eberhard Karls Universität Tübingen, Sigwartstraße 10, D-72076 Germany

Received 23 December 2003; received in revised form 10 August 2004; accepted 23 August 2004

Available online 23 November 2004

Abstract

Of the several vein types with elongate crystals, we distinguish a class of veins with well-developed fibres, exposed at Oppaminda Creek (South Australia). These calcite veins are characterised by very limited competition between growing crystals, which leads to the development of fibrous crystals with smooth boundaries and which can attain extreme length–width ratios. Fibres are often curved and track the opening trajectory. The veins are also characterised by their outwards, antitaxial growth, starting from a narrow median zone. These median zones contain wall rock inclusions and a distinctly different, non-fibrous internal microstructure. Such veins continue growing as long as extension is suitably oriented relative to the vein orientation. Multiple, cross-cutting vein sets can thus grow simultaneously and can together track over 90° rotation of the fibre growth direction.

The veins formed by calcite precipitation on both their outer surfaces. We suggest that the term ‘antitaxial’ should be redefined as applying only to those veins that have two simultaneous growth planes at their outer surfaces. Antitaxial veins grow without further fracturing, which sets them apart from other veins that grew by precipitation inside a crack, and which only have one single growth plane at the time.

The veins at Oppaminda Creek are about 585 Ma in age, and therefore formed at an estimated 4–6 km depth. Scanning electron microscope observations revealed about 1- μ m-sized structures, which we interpret as fossils of microbes that lived inside the veins at the time of their formation, and which may even have played a role in the vein formation. These structures would represent the first finds of fossilised life forms of such a combined age and depth.

© 2004 Elsevier Ltd. All rights reserved.

Keywords: Fibrous veins; Antitaxial veins; Fossil microbes; Flinders Ranges; Neoproterozoic

1. Introduction

Veins are useful and classical textbook tools to help unravel deformation histories of their host rocks (e.g. Ramsay and Huber, 1983; Twiss and Moores, 1992; Passchier and Trouw, 1996; Oliver and Bons, 2001). Their shape and orientation are indicators of palaeostrain orientations, their composition points to diagenetic or metamorphic conditions and fluid compositions, while fluid inclusions record composition, pressure and temperature of vein forming fluids. Structural geologists also rely on the internal microstructure to refine the tectonic analysis of veins (Durney and Ramsay, 1973; Ramsay and Huber,

1983; Beutner and Diegel, 1985; Cox, 1987; Etchecopar and Malavieille, 1987; Williams and Urai, 1989; Foxford et al., 2000; Koehn and Passchier, 2000, amongst many others). Fibrous veins, especially, can record opening trajectories of veins in great detail (Durney and Ramsay, 1973; Casey et al., 1983; Ramsay and Huber, 1983; Passchier and Urai, 1988; Spencer, 1991).

In the literature, the term ‘fibrous’ usually refers to any vein with distinctly elongate crystals. This can be the case if the vein is filled with a normally fibrous mineral, such as asbestos. In most cases, however, veins are filled with minerals such as quartz or calcite, which normally do not have a fibrous habit. To correctly interpret vein structures, it is of importance to clearly distinguish between different types of fibres (Bons, 2000, 2001):

(1) Stretched crystals (Durney and Ramsay, 1973) form by

* Corresponding author. Tel.: +49-7071-2976469; fax: +49-7071-5059
E-mail address: paul.bons@uni-tuebingen.de (P.D. Bons).

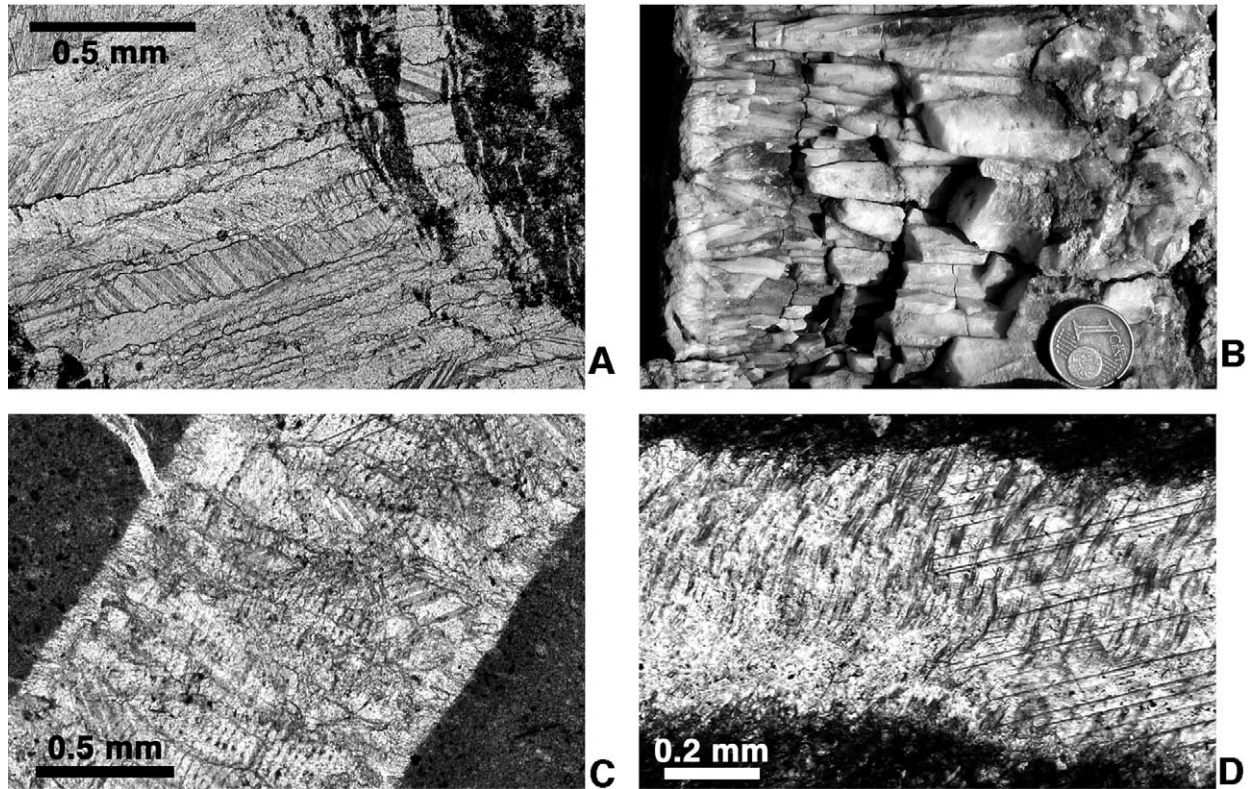


Fig. 1. (A) Stretched crystal vein in carbonate-rich layer from Oppaminda Creek. Wall rock inclusions show the incremental growth in steps of about $20\ \mu\text{m}$ at a time. (B) Asymmetric elongate blocky calcite vein showing growth to the right only (stratigraphically upwards) and strong growth competition. Image spans the entire vein width. Coin for scale is 16 mm. Upper Cretaceous limestones, near Molinos, Teruel Province, Spain. (C) Wall rock parallel inclusion bands, with $\sim 30\ \mu\text{m}$ spacing, in a stretched-crystal calcite vein. Beach boulder from the Mt. Gottero Unit (Marroni, 1991), near Sestri Levante, Italy. (D) Ghost fibres in a calcite vein. Elongate inclusions that form consistent curved traces across the vein indicate the opening trajectory. Neoproterozoic Skillingalee Dolomite Unit, Arkaroola campground, South Australia.

incremental stretching of vein crystals (Fig. 1A). The crystals typically span the whole width of a vein and usually have serrated boundaries (Ramsay, 1980; Hilgers and Urai, 2002). Because stretched crystals connect material points on the vein surface that were originally adjacent to each other, stretched crystals show the finite opening vector of a vein, but not its incremental opening path or trajectory.

- (2) Elongate–blocky crystals form when growth competition leads to some crystals outgrowing others, leading to blade-like shapes in thin section (Fisher and Brantley, 1992; Bons, 2001) (Fig. 1B). Growth competition occurs when crystals grow into a fluid-filled space, such as a fracture (Mügge, 1925; Durney and Ramsay, 1973). Growth competition is suppressed when the fracture has a rough surface and is very narrow (Urai et al., 1991). Hilgers and Urai (2002) estimated that growth competition is fully inhibited when the crack width is less than about $10\ \mu\text{m}$. The growth direction of crystals is not only determined by the direction of (incremental) crack opening, but also by the crystallographically controlled growth competition (Hilgers et al., 2001). The average growth direction may

therefore differ from the vein opening direction: the crystals do not necessarily follow the opening trajectory (Cox, 1987; Urai et al., 1991; Koehn and Passchier, 2000; Bons, 2001; Hilgers et al., 2001).

- (3) Some veins contain crystals that show little or no increase in their width along their growth direction. The crystals have a strongly fibrous shape, even when the minerals forming them do not usually have a fibrous habit. This implies that growth competition is suppressed or completely disabled (Mügge, 1928; Urai et al., 1991; Bons and Jessell, 1997; Hilgers and Urai, 2002). Fibres are often curved without any bending of the lattice, indicating that the fibres grew in a curved shape, following the opening trajectory (Durney and Ramsay, 1973). Hilgers and Urai (2002) make no sharp distinction between elongate–blocky crystals and strongly fibrous crystals, but regard the latter as an end-member case where growth competition is suppressed. Bons and Jessell (1997) and Bons (2000) argued that very fibrous crystals should be distinguished from elongate–blocky crystals. They argue that very fibrous crystals do not grow into an open fracture as elongate–blocky crystals do, but on

a surface that maintains mechanical cohesion (Mügge, 1928).

Veins can also be classified according to the growth direction of these crystals (Durney and Ramsay, 1973). The three main classes are:

- (a) Stretched veins (Durney and Ramsay, 1973) or ataxial veins (Passchier and Trouw, 1996) (Fig. 2A). Stretched veins form by the repeated opening and sealing of fractures that do not occupy the same position within the growing vein. The crystals in stretching veins are stretched crystals.
- (b) Syntaxial veins (Fig. 2B and C) are defined by Durney and Ramsay (1973) as those veins where “the vein filling is an overgrowth on the original wall rock grains and takes place in optical continuity with them”. Contrary to stretching veins, growth takes place on a single plane with a consistent position within the vein, often somewhere in the middle, but sometimes completely on one side (Fig. 1B). It is generally assumed that this plane is a fracture that is sealed by inward growth on both surfaces of that fracture.
- (c) In antitaxial veins (Fig. 2D) the crystals “are in optical continuity across the vein and appear to grow from a median suture line toward the walls” (Durney and Ramsay, 1973). This implies that antitaxial veins have two growth planes, located between the vein and the wall rock.

The definition of syntaxial and antitaxial veins is based on the growth direction of vein crystals relative to the wall rock. This definition leads to ambiguity in the case of veins that grow from one side to the other (Fig. 1B). Such a vein would be syntaxial on one side and antitaxial on the other. Clearly, this situation is unsatisfactory. Bons (2000) therefore suggested that the terms syntaxial and antitaxial be redefined. Syntaxial veins have *one single* growth plane with a consistent position within the vein. Antitaxial veins have *two simultaneous* growth planes, located on the outer surfaces of the vein. This definition avoids any ambiguity.

Using this definition, some veins that have been described as ‘antitaxial’ should now be termed ‘syntaxial’ (e.g. fig. 5 in Foxford et al., 2000). Antitaxial veins are normally very fibrous and the fibres are often curved and tend to accurately follow the opening trajectory. They are commonly formed by calcite in dark shales (Passchier and Urai, 1988; Williams and Urai, 1989; Elburg et al., 2002; Hilgers and Urai, 2002), but can also be composed of other minerals, such as quartz or gypsum.

The formation of fibrous veins in general is usually attributed to the crack-seal mechanism of Ramsay (1980), which envisages vein opening to occur in small crack-opening increments, which are followed by filling or sealing of the narrow crack with mineral precipitate. Commonly cited indicators for crack-sealing are wall-rock parallel inclusion bands (Fig. 1C) and ghost fibres (Fig. 1D) (Ramsay, 1980; Cox and Etheridge, 1983; Cox, 1987; Passchier and Trouw, 1996; Lee et al., 1997). However, several recent publications have put a crack-seal origin for fibrous, antitaxial veins in doubt (Fisher and Brantley, 1992; Bons and Jessell, 1997; Bons, 2000; Oliver and Bons, 2001). Even the classical indicators for crack-sealing, such as inclusion trails and bands, have been questioned by Wiltshko and Morse (2001) and Means and Li (2001). They argue that banding may result from fluctuations in fluid chemistry and does not necessarily represent crack-seal banding.

It has been already recognised by Mügge (1928) that growth competition must be inhibited to enable the growth of fibrous quartz or calcite. Urai et al. (1991) argued that growth competition could be inhibited during crack-sealing if crystal boundaries lock on to asperities on the wall rock. This was modelled by Hilgers et al. (2001), using the numerical model of Bons (2001), showing that the crack must be thinner than about 10 μm , if such veins were to grow by the crack-seal mechanism. Growth competition is also inhibited if growth occurs at an essentially closed surface whereby vein opening is enabled by the force of crystallisation of the growing crystals (Bons and Jessell, 1997; Means and Li, 2001; Wiltshko and Morse, 2001).

Most of the works cited above provide geometrical or kinematic descriptions of the formation of vein textures. It is

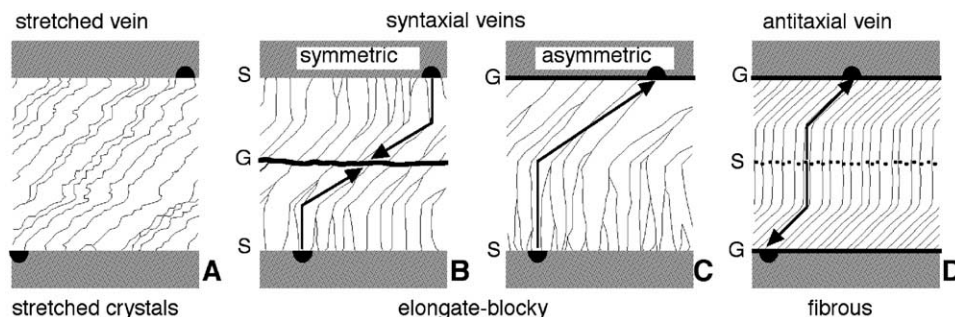


Fig. 2. Different vein types classified by the growth direction of vein-filling crystals. ‘S’ is the plane where growth of crystals inside the vein started, and ‘G’ is the plane where current growth takes place. Black half-circles indicate two points on the vein surface that were originally adjacent to each other. (A) Stretched or ataxial vein, with stretched crystals. (B) Syntaxial vein, where growth occurred from the wall rock towards the middle of the vein. (C) Asymmetric syntaxial vein, with growth fully on one side of the vein. (D) Antitaxial fibrous vein, where fibres grow outwards from the middle of the vein.

less clear under which dynamic and geochemical conditions the various vein types may form. It is still especially unclear why and when antitaxial fibrous veins form if the growth surfaces are essentially closed (in the sense that there is a mechanical continuity across the vein and wall rock interface). Although Wiltschko and Morse (2001) showed that a supersaturated pore fluid can cause antitaxial fibrous growth, they do not indicate the cause for such a supersaturation, nor under what circumstances such a supersaturation would lead to antitaxial fibrous growth. The antitaxial fibrous vein growth in the experiments by Means and Li (2001) was driven by evaporation, but they could not indicate what the equivalent process would be in a rock.

By far the most literature on vein microstructures deals with the more common syntaxial elongate blocky veins. Fibrous, antitaxial vein growths (in the strict sense used here) have received less attention, with only one recent systematic description of this vein type (Hilgers and Urai, 2002). The closely related antitaxial, fibrous pressure fringes, on the other hand, have again been extensively investigated and described (Pabst, 1931; Elliot, 1972; Aerden, 1996; Kanagawa, 1996; Koehn et al., 2001, 2003). Before any genetic interpretation of fibrous antitaxial veins can be made, it is necessary to describe their morphology and characteristics in detail. A population of such veins is described in this paper, focussing on aspects that are particular to antitaxial fibrous veins, to show that such veins form a distinct class that does not form by crack-sealing, but by growth on both their closed outer surfaces. We also show indications that hyperthermophile microbes may perhaps have played a role in their formation.

2. Antitaxial fibrous veins at Oppaminda Creek

2.1. Regional setting

The veins are found a few kilometres south-east of Arkaroola Village (Northern Flinders Ranges, South Australia) in the Tindelpina Shale member, which is the lowermost member of the Tapley Hill Formation (both defined by Coats in Thomson et al. (1964)) (Fig. 3), which is in turn part of the Neoproterozoic–Cambrian Adelaidean Sequence (Coats and Blissett, 1971; Preiss, 1987; Drexel et al., 1993; Wingate et al., 1998). The Tindelpina Shale Member represents a widespread transgression at ~700–750 Ma, shortly after the second Sturtian glaciation event (Preiss, 1987). It consists of finely laminated dark carbonate and pyrite-rich shale with a high organic content (McKirdy et al., 1975). Decimetre-scale dolomite beds occur at the base, and centimetre-scale dolomitic siltstone layers occur dispersed throughout the unit. Massive pale-yellow dolomite beds overlie the shales (Fig. 3C).

The Adelaidean Sequence was deposited during a succession of localised rifting and basin-wide subsidence events (Coats and Blissett, 1971; Preiss, 1987; Drexel et al.,

1993; Mildren and Sandiford, 1995). Faults associated with the syn-sedimentary rifting are long-lived. Some have been continuously reactivated, such as the currently active Paralana Fault. Diapiric mobilisation of the lowermost Adelaidean units, in particular the evaporitic Wywyana Formation, occurred throughout the Flinders Ranges, during deposition of the Adelaidean Sequence (Preiss, 1987), but no evidence for such activity is found near the vein locations. Evidence for a basin-wide fluid flow event at $\sim 586 \pm 30$ Ma, about when the upper Wilpena Group was being deposited, was first reported by Foden et al. (2001). Elburg et al. (2002) carried out a detailed geochemical analysis of the Oppaminda Creek veins and published 10 equilibrium ages, the ages at which the Sr fraction from the leached host rock would be in isotopic equilibrium with the vein Sr. These ages range from 497 to 622 Ma, which appears to support that the veins formed during the late Neoproterozoic 586 ± 30 Ma fluid flow event of Foden et al. (2001). The known timing of vein formation, and the absence of any known significant deformation or folding before that time, allows us to estimate the depth of vein formation, which is approximately the local height of the stratigraphic column from the Tindelpina Shale Member to the upper Wilpena Group. Both the isopach maps of Preiss (1987) and a profile constructed from the geological map of Coats and Blissett (1971) indicate that the veins formed about 4–6 km below the seafloor (not corrected for compaction of overlying sediments).

Folding during the ~500 Ma Delamerian Orogeny formed the presently dominant structures and outcrop patterns (Coats and Blissett, 1971; Preiss, 1987; Drexel et al., 1993). The Delamerian Orogeny produced kilometre-scale open folds, with locally E–W- to NE–SW-trending axial planes (Fig. 3A). Overall shortening was minor: ~20% south of Arkaroola Village (Paul et al., 1999). The Oppaminda Creek outcrops lie in a gently (20–25°) west-dipping hinge of the Arkaroola Syncline (Figs. 3 and 4B). The Adelaidean rocks close to the (?Palaeo-) Mesoproterozoic Mt. Painter Inlier north of Arkaroola Village were metamorphosed and developed a cleavage during the Delamerian Orogeny (Coats and Blissett, 1971; Drexel and Preiss, 1995; Paul et al., 1999; Elburg et al., 2001). Cleavage development quickly dies out with decreasing metamorphic grade south of Arkaroola Village, and no cleavage developed at Oppaminda Creek. McLaren et al. (2002) argued that the Delamerian Orogeny was associated with a ~70 My period of elevated temperature in the area, lasting until the late Ordovician. However, Elburg et al. (2003) showed that the Delamerian event was in fact not long-lived, but followed by a hydrothermal and magmatic event at ~440 Ma, which resulted in the intrusion of the British Empire Granite within the Mt. Painter Inlier, and widespread actinolite–tremolite–scapolite alteration in the Lower Adelaidean units close to the Inlier. This alteration did not, however, extend as far south as the Oppaminda Creek outcrops.

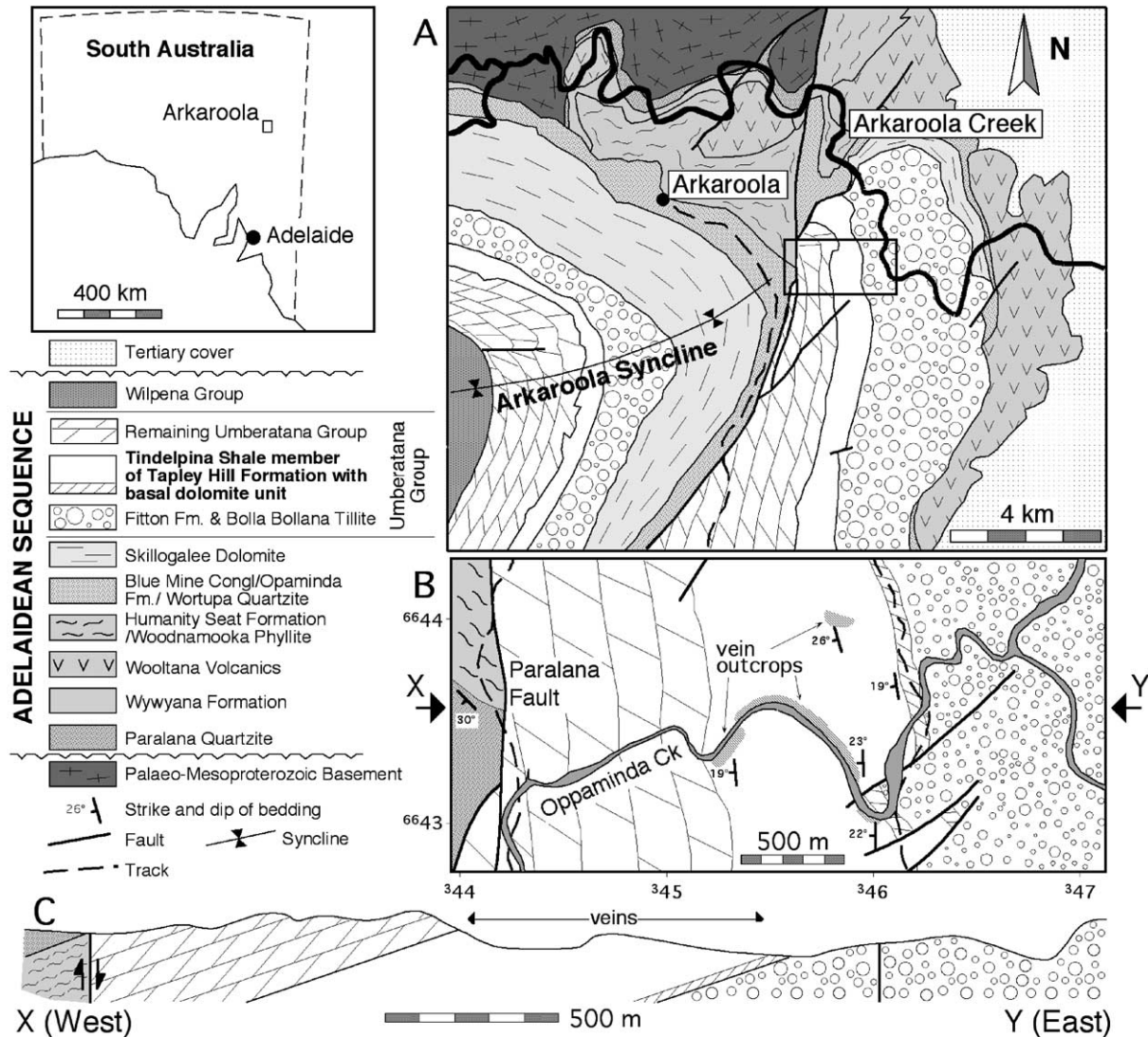


Fig. 3. Geology of the Oppaminda Creek outcrops, near Arkaroola Village, South Australia (inset). (A) Geology of the region, after Coats and Blissett (1971). (B) Map of the local area (rectangle on (A)) around the outcrops in Oppaminda Creek and adjacent gullies. (C) E–W profile through the area shown in (B).

2.2. Field occurrence of the veins

Antitaxial fibrous veins are abundant in the dark shale lithology of the Tindelpina Shale Member, but are absent in other lithologies and adjacent units. The veins consist of calcite with only minor Fe- and Mg-carbonate (<2% each) (Elburg et al., 2002). Pyrite and Cu-sulphide are minor constituents of all veins, but macroscopically visible crystals are rare.

The veins show a wide range in shape, from metres long thin sheets to short (centimetre–decimetre) lenses (Fig. 5A–C). Vein widths are generally below 1–2 cm, but can reach up to almost 10-cm (Fig. 5D). Sheet-like veins tend to form multiple connecting sets. An important observation is that differently oriented veins very rarely cross each other, but normally form T-junctions (Fig. 5B and C). This is in contrast to typical fracture-fill veins with elongate–blocky

vein fillings, where one vein (set) normally cuts through another older vein (set).

Bedding dips about 20–25° to the WSW in and near Oppaminda Creek. The sedimentary layering is locally slightly folded in asymmetric, mostly decimetre-scale open folds, with a fold axis that plunges ~5° to the NW (Fig. 4B). Since some straight veins cut these folds and the fold axis is up to 90° to Delamerian fold axes, this folding must have coincided with or preceded the ~585 Ma vein formation event. This folding thus represents an early, hitherto unknown, but very minor deformation event. Vein orientations vary greatly, but their poles define a broad great circle, oriented 200/60 (Fig. 4C). This is not the result of folding, as the veins are not significantly folded or deformed, and the host rock sedimentary layering has a fairly constant orientation.

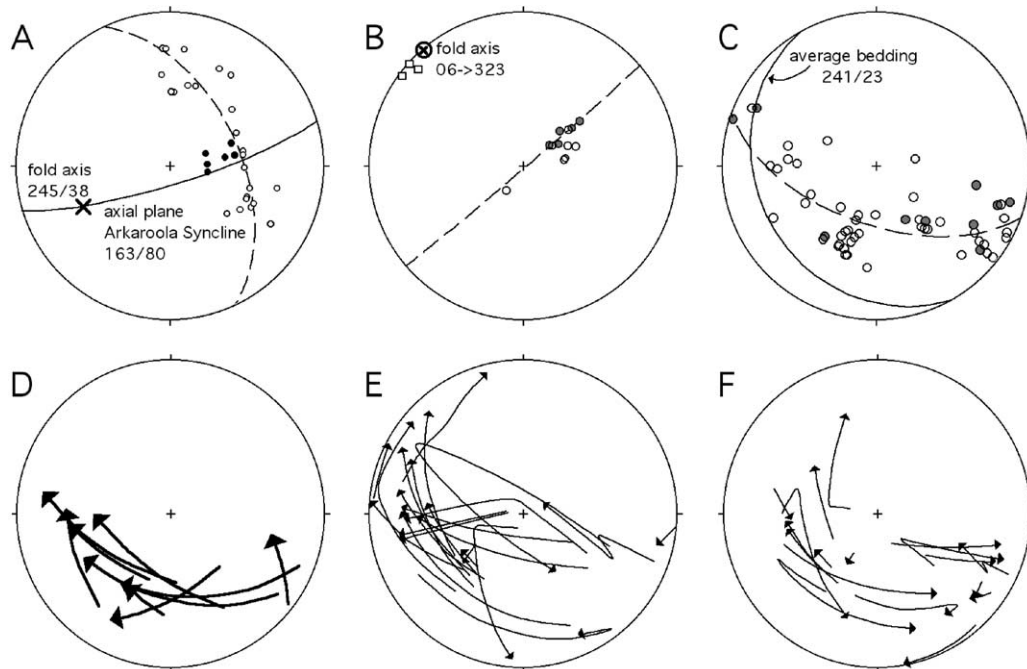


Fig. 4. Orientations in equal area stereoplots. (A) Orientations of poles to bedding in Adelaidean formations south of Arkaroola (from the geological map of Coats and Blissett (1971)) for the area shown in Fig. 3A. Twenty-four data points taken west of the Paralana Fault (white dots) and six east of the fault (black dots). Data lie on a great circle, with the fold axis at 245/38. Orientation of the axial plane (163/80) determined from the fold axis and the surface trace of the axial plane, west of the Paralana Fault. (B) Poles to bedding (white dots, 7 \times) and axes of minor folds (squares, 3 \times) at the Oppaminda Creek outcrops. Grey dots (5 \times) are measurements of bedding along a single, open, less than metre-scale fold, giving a fold axis at 323/06. (C) Poles of blocky (filled dots, 10 \times) and fibrous (open dots, 44 \times) from area shown in Fig. 3B. Veins lie on a broad great circle (dashed line) with orientation 200/59. (D) Age relationships between nine intersecting vein sets. Start of arrow at pole of older vein set and end of arrow at younger one of the pair. General trend is from steeply NW dipping veins, towards moderately NE dipping veins. (E) Traces of fibre growth direction. Each arrow starts at the oldest fibre growth direction (middle of vein) and ends at the youngest growth direction. (F) Traces of extension direction, constructed with the 'convinc' method of Durney and Ramsay (1973).

2.3. Fibres

The large majority of the veins is fibrous and antitaxial (Fig. 6A). Fibres range in width from a few microns to several hundreds of microns. However, blocky veins also occur and some veins show a stage of fibrous growth and one of blocky growth (Fig. 6B). Where blocky crystal growth preceded fibrous growth, the blocky texture forms a usually narrow layer in the middle of the vein, from which fibres subsequently grew outwards in both directions (Fig. 7). In other cases blocky growth succeeded fibrous growth, in which case the blocky part of the vein can be up to centimetres in width. Fully blocky veins have the same spread in orientation as completely or dominantly fibrous veins (Fig. 4C). Nine unambiguous relative age relationships (cf. fig. 13.1 in Ramsay and Huber, 1983) between vein sets were recorded (Fig. 3D). Older vein sets are steeply NW-dipping, while the younger ones tend towards a NE-dip.

Fibres have smooth boundaries (Fig. 6C), contrary to 'fibres' in some stretched crystal veins, which may show distinctly serrated boundaries. Fibres are curved and follow the opening trajectory: they connect points on the vein surface that were originally adjacent to each other and the curvature indicates the progressive widening direction of the vein. Curvature is not due to bending, as the lattice is not

bent where fibres are curved (see Williams and Urai, 1989). Minor deformation of the veins has occurred, either during or after vein growth, as vein calcite is twinned.

Fibres tend to commence their growth at right angles to the vein surface, indicating that the veins initially formed perpendicular to the current direction of maximum extension. The trend in Fig. 4D can thus be interpreted as the evolution of the maximum extension direction. Fibres are usually curved as they changed their growth direction as the vein widened. Fig. 4E shows fibre orientations, plotted on a stereoplot, where for each vein at least two orientations were measured: early and late growth directions. A consistent picture emerges with growth directions gradually changing from plunging to the SE, steepening, then turning towards a westward plunge and finally to an approximately horizontal NW–SE orientation. This trend is consistent with the one derived from vein age relationships (Fig. 4D). Fibres in individual veins usually only track part of the whole evolution, depending on the vein orientation and point of time that the veins started growing. If it is assumed that fibres grow in the direction of maximum extension (the 'standard' method of Durney and Ramsay (1973); see also Ramsay and Huber, 1983), the fibres track the reorientation of the strain field that ended in NW–SE extension. Fibres, however, only track the displacement direction of the vein

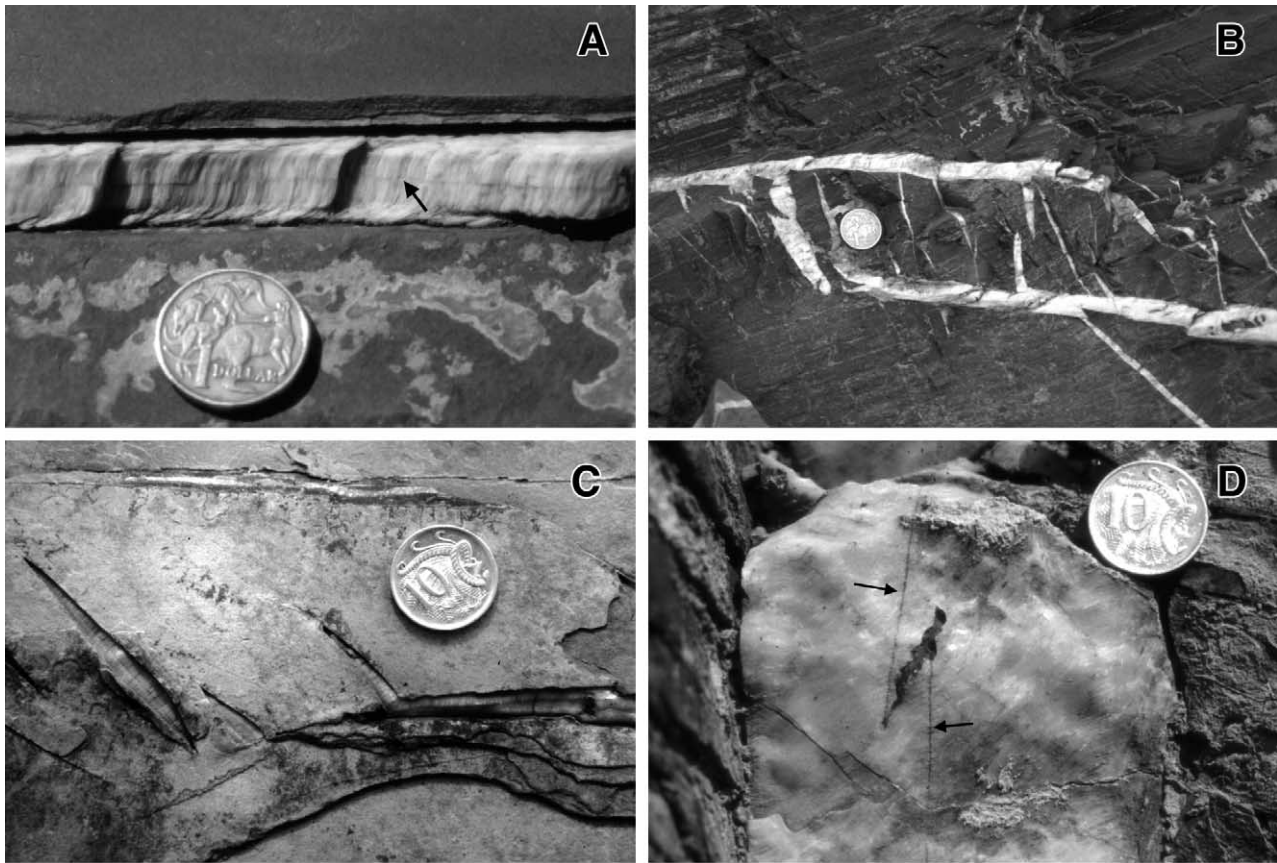


Fig. 5. (A) Straight symmetrical antitaxial fibrous vein with curved fibres and a visible median zone in the middle (arrow). Coin for scale 24 mm. (B) Stepping structure between two gently dipping veins and a vein that dips steeply to the right (lower-right corner). Notice that all vein-intersections are T-junctions. Coin for scale 24 mm. (C) Individual lenticular veins (left) and branching veins (right), again exhibiting T-junctions. Coin for scale 23 mm. (D) Photograph of largest vein found in the area. The vein has a distinct median zone (arrows). A grey wall rock sliver in the middle shows that the vein formed by amalgamation of slightly offset veins. Coin for scale 23 mm.

walls relative to each other, which must not necessarily coincide with the bulk maximum extension direction. According to the ‘convinc’ method of Durney and Ramsay (1973) the actual extension direction bisects the angle between the fibre direction and the vein pole. Extension direction paths constructed with the ‘convinc’ method are plotted in Fig. 4F. The individual extension direction paths show less consistency, but a general trend toward a gently SE-plunging maximum extension can be discerned. The ‘convinc’ method relies on the assumption that there is no stretching parallel to the veins. This assumption probably does not hold for the multiple and differently oriented vein sets at Oppaminda Creek. In such a case, resembling the ‘chocolate tablet’ structures of Ramsay (1967) and Ramsay and Huber (1983), the ‘standard’ method (fibres follow extension direction) is preferred, according to Durney and Ramsay (1973).

Both methods for estimating the extension suggest a large rotation of the extension direction, which is difficult to explain as being due to rotation of the limb of the Arkaroola Syncline in a non-rotating stress field, since the limbs only rotated a few tens of degrees at the most. If the veins are

indeed pre-Delamerian (Elburg et al., 2002), they would have rotated passively along with the south-eastern limb of the syncline.

Although the high length/width ratio of the fibres indicates that growth competition between individual fibres is suppressed, there is some increase in average fibre width as growth proceeds. Initial fibre width appears to be controlled by the grain size and internal structure (twins) of the seeding crystals in the median zone (see below), but also possibly by the roughness of the initial vein surface. There is virtually no increase in average fibre width along straight fibre sections, but average fibre width increases where fibres are curved. At the edge of the vein (Fig. 6D and E), fibre boundaries lie on asperities, typically vertices of quartz crystals that form a selvedge on the vein rim (see below), as described by Hilgers and Urai (2002). An increase in width when opening direction changes can be explained by changing in the locking sites of fibre boundaries, as was observed in numerical simulations (fig. 2 of Bons, 2001). With the curvature and average width of fibres it is possible to determine growth isochrons and to reconstruct the opening of a vein (cf. Ramsay and Huber, 1983).

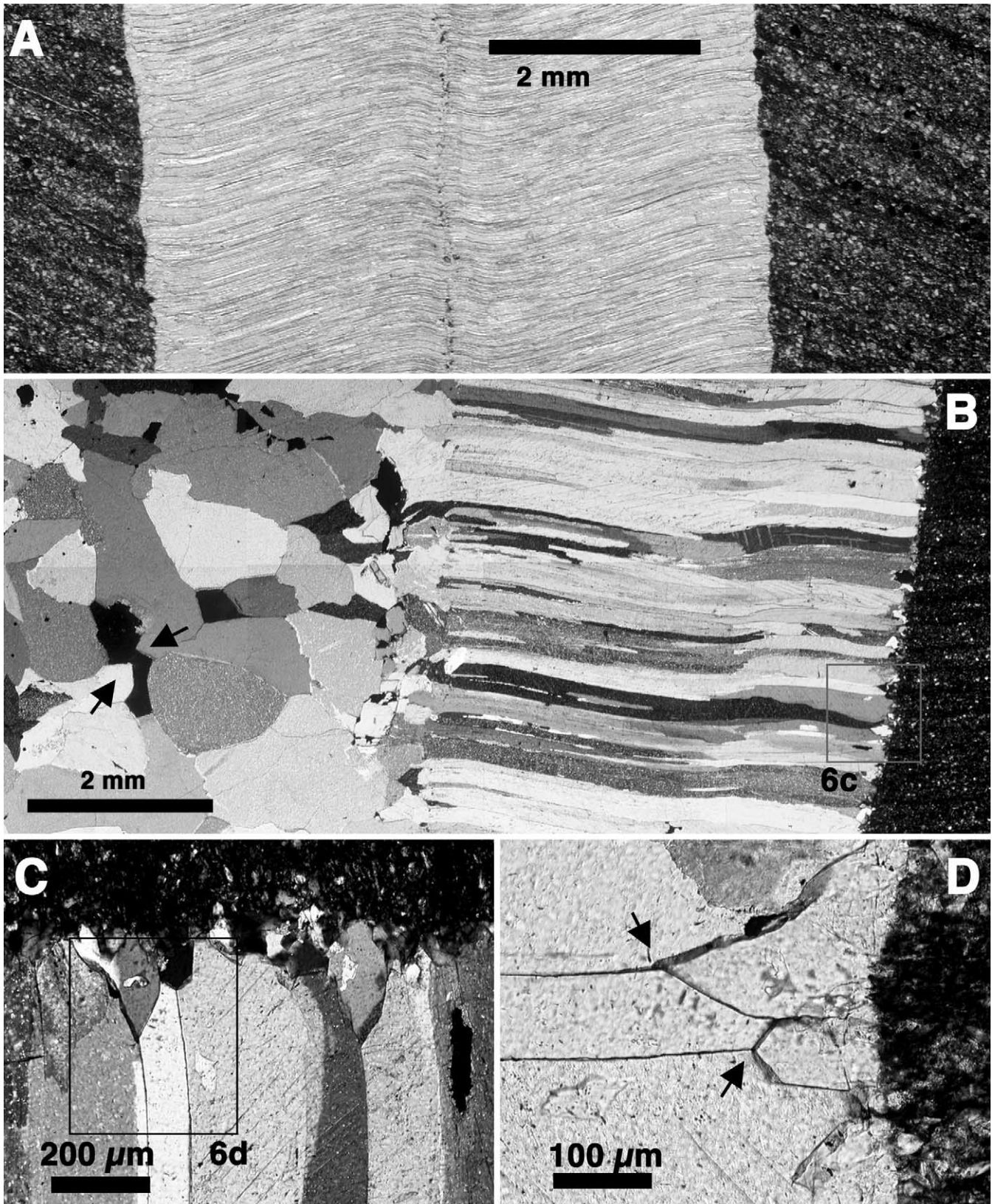


Fig. 6. Microstructures of fibrous veins from Oppaminda Creek. (A) Symmetrical antitaxial fibrous calcite vein (same as Figs. 7A and 8), oblique to sedimentary lamination in shale. (B) Composite vein with an antitaxial fibrous part (right) where fibres grow to the right and a syntaxial part (left) where crystals grew toward the left. Remaining voids show euhedral crystal facets (arrows). The wall rock surface is lined by a thin rim of quartz crystals that grew outwards from the wall rock, into the vein. (C) Enlargement of rectangle in (B), showing quartz rim in detail. Notice the smooth fibre boundaries. (D) Enlargement of rectangle in (C), showing that fibre boundaries lock onto tips of quartz crystals (arrows).

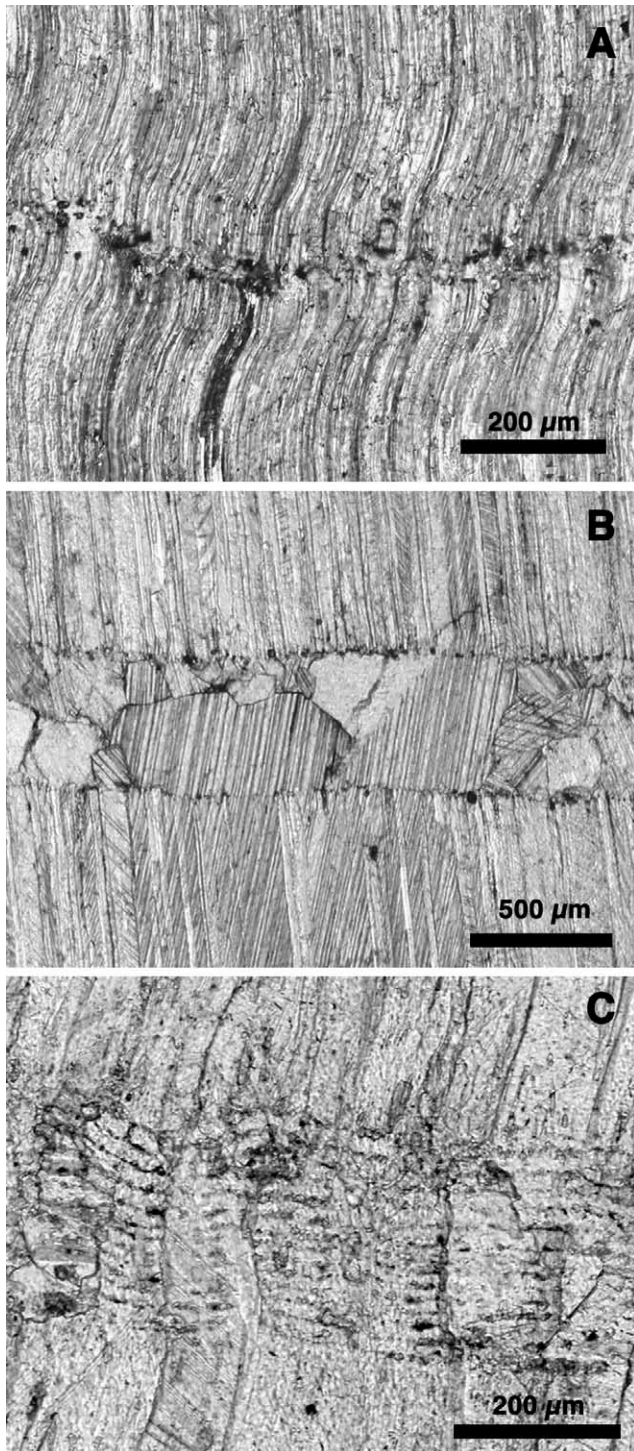


Fig. 7. Micrographs of median zones in antitaxial fibrous calcite veins (A) $\sim 40 \mu\text{m}$ wide zone, marked by dark wall rock inclusions, in the middle of a finely fibrous vein, shown in Fig. 6A. Crossed polars. (B) 0.5 mm wide median zone with a distinctly non-fibrous internal microstructure. Sample from Oppaminda Creek. (C) 250 μm wide median zone with parallel inclusion bands, which are absent in the fibrous crystals on either side of the median zone. Beach boulder from the Mt. Gottero Unit (Marroni, 1991), near Sestri Levante, Italy.

2.4. Median line/zone

One characteristic of antitaxial veins is that they are of a different composition than their host rock (Durney and Ramsay, 1973): in this case calcite veins in a shale that only contains a few percent of calcite. The host rock is therefore not the substrate on which vein crystals grew. Instead, antitaxial veins contain a planar zone, often roughly in the middle, where the vein-forming mineral first nucleated (Fig. 7). This zone is usually termed the ‘median (suture) line’ (Durney and Ramsay, 1973), but ‘median zone’ is used here because the zone always has a finite width, which can range from a few micrometres only, to several millimetres. Median zones can be recognised by (a) wall rock inclusions (Fig. 7A), and (B) a different, non-fibrous texture, usually (elongate) blocky (Fig. 7B), but ‘crack-seal’-like inclusion bands can also occur (Fig. 7C). The difference in texture indicates that crystal growth inside the median zone occurred by a different mechanism from subsequent fibrous growth on both sides of the median zone. The (elongate) blocky, or stretched-crystal textures in the median zones indicate that median zones were thin cracks, which were filled in one or more events.

Thanks to the tracking capability and optically visible growth zonation in the veins, it is possible to reconstruct the veins at the time before antitaxial fibrous growth commenced (Fig. 8). Before fibrous growth commenced, median zones already spanned the entire length of veins. Therefore, there is no lateral propagation of veins during fibrous growth. This implies that the overall geometry and orientation of veins is determined by the process that produced the median zones. The blocky texture, sometimes with parallel inclusion bands, suggests that this process was brittle failure. Subsequent antitaxial fibrous growth only widened the existing narrow veins.

2.5. Quartz rim

Antitaxial fibrous veins in shales tend to have a narrow quartz (\pm chlorite) selvage (Elburg et al., 2002; Hilgers and Urai, 2002) (Fig. 6C), consisting of small quartz crystals that grew out from the wall rock (syntaxial growth). The width of this selvage is quite constant along a vein, independent of the width of that vein. At the vein tip, the vein may thus consist mostly of quartz, rather than calcite. Quartz precipitate can also be found at junctions of veins, and sometimes within the median zone. As was pointed out by Hilgers and Urai (2002), the quartz selvages play an important role in the fibrous microstructure, as fibre-boundaries tend to lock on tips of quartz crystals (Fig. 6D). The quartz crystals thus play a role in controlling fibre width, as well as perhaps the size of the seed crystals.

2.6. Blunt and frilly vein tips

Veins abruptly end, or change their shape and

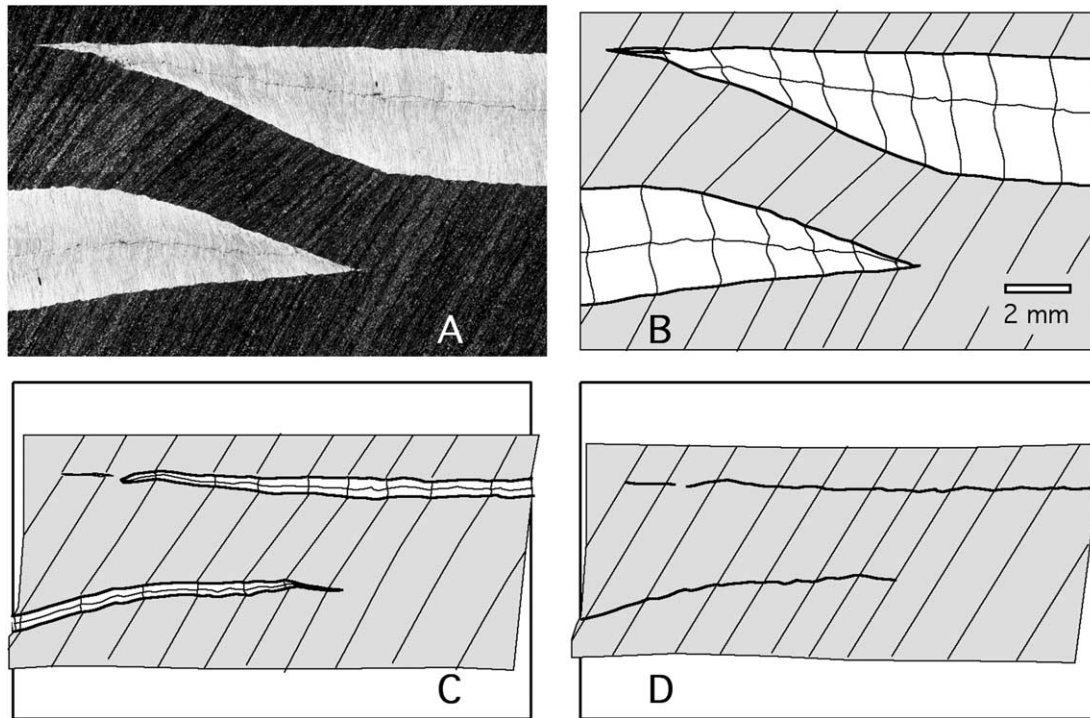


Fig. 8. (A) Micrograph of a wall-rock bridge between two vein tips. Sedimentary lamination in the shale dips steeply to the left and is rotated within the bridge, due to the widening of the two veins. (B) Drawing of the same situation, showing the current vein, the lamination and the fibre orientations. Fibres track the opening trajectory. (C) Reconstruction of the veins to the stage where the veins were about 1 mm wide. (D) Reconstruction of the veins at the start of fibrous growth, when only the median zones were present. Median zones already span the entire vein length at this starting stage and veins did not propagate laterally from this point onwards.

microstructure, where they intersect a coarser-grained carbonate layer (Fig. 9). Where a vein abuts against a carbonate layer, strain within that layer is distributed and achieved by stretching of individual grains or a number of small stretching veins. In the latter case, the veins ends are frilly. Veins within carbonate-rich layers are never antitaxial fibrous, but of the blocky or stretched-crystal type. Similar vein-ends are also found in antitaxial fibrous veins from other locations around the world (Passchier and Urai, 1988; Hilgers and Urai, 2002).

2.7. SEM observations

Polished blocks of the veins were examined with a LEO-Gemini 1450VP scanning electron microscope (SEM) at acceleration voltages between 20 and 30 kV and a JEOL JSM-6340F field-emission SEM at 2 kV. Etched samples were treated with 0.1 M HCl for 30 s to remove the outer $\sim 25 \mu\text{m}$ of calcite, in order to exclude any possible recent surface contamination and to reveal inclusions *inside* the calcite fibres. The etching process was terminated by rinsing the samples with filtered distilled water. After drying, the samples were sputter-coated with a thin conductive gold layer, except for the one sample for the field-emission SEM.

Fibre surfaces are smooth on the micrometre-scale, and fibre boundaries are tight, $\ll 1 \mu\text{m}$ in width (Fig. 10A). Fig. 10B shows a sample after etching, which removed the

surface and penetrated deep along fibre boundaries. The etching revealed groups of small, $\sim 1 \mu\text{m}$, globular and rod-shaped objects that were embedded within the fibre calcite (Fig. 10C–F). The rough etch patterns that surround the objects are evidence that these objects were embedded *within* the calcite (Fig. 10C). These objects strongly resemble known mineralised micro-organisms, such as those reported by Folk (1999) and Westall et al. (2000). Morphology is, however, a controversial and hotly debated indicator of biogenicity, especially in view of claims of life on Mars and early in the Archaean on Earth (Schopf, 1993; McKay et al., 1996; Westall et al., 2001; Brasier et al., 2002; García-Ruiz et al., 2002, 2003). In light of this controversy, we carefully examined the structures in the calcite fibres to determine whether they are truly biogenic, and not abiogenic artefacts. Fig. 10E shows two rod-like objects linked together, indicating cell division. Another case of possible cell division was found in an object that showed two parallel girdle-like wall-bands (Fig. 10F), known to form in micro-organisms in the early stage of division (Madigan et al., 2000). In some cases, the objects are associated with thin strings with knots (Fig. 10E), reminiscent of the *cannulae* of the hyperthermophile modern archaea *Pyrodictium* (Stetter et al., 1983; König et al., 1988) or the bacterial filaments reported by Thomas-Keprta et al. (1998).

Whether these structures are biogenic must be critically

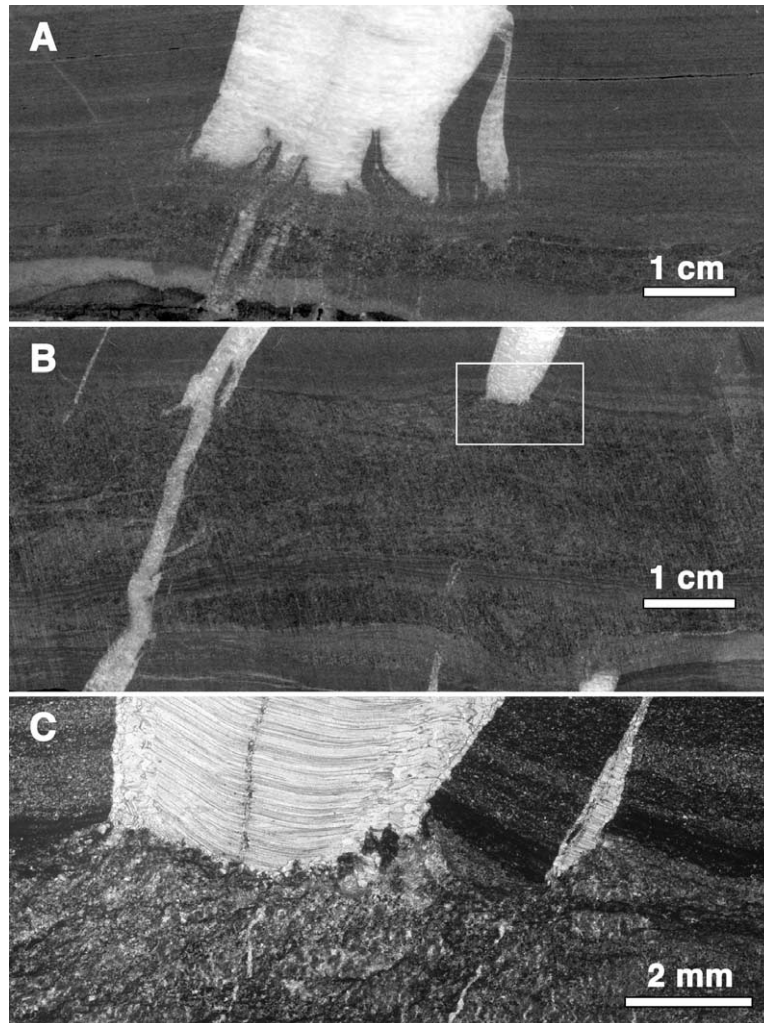


Fig. 9. (A) Scan of a polished slab, showing an antitaxial fibrous vein, abutting a carbonate-rich layer. Veining inside the carbonate-rich layer is diffuse and of the stretched-crystal type. (B) Scan of a polished slab, showing antitaxial vein (right) that ends abruptly against a carbonate-rich layer. The vein on the left intersects the layer and has blocky crystals along its whole length. Within the shale (top and bottom), the blocky core is rimmed on both sides by fibrous calcite, which is completely absent within the carbonate-rich layer. (C) Micrograph of rectangle in (B), showing the fibrous vein ending against the carbonate-rich layer. Extension within that layer is distributed in numerous thin veinlets.

considered, because non-biogenic processes can produce remarkably life-like structures (Westall, 1999; Brasier et al., 2002; García-Ruiz et al., 2002, 2003). We present the following arguments in support of a biogenic origin for the globular and rod-shaped structures:

- (1) The size range of the structures is about 0.5–2 μm , typical for bacteria and archaea (Pirie, 1973; Koch, 1996; Nealson, 1997). Although non-biogenic structures may strongly resemble fossil micro-organisms, they develop in a variety of sizes (García-Ruiz et al., 2002).
- (2) The occurrence in colonies and groups is typical for life forms and is also observed in our samples.
- (3) Biomorphic globules, rods, spirals and strings or filaments may all form non-biogenetically (García-Ruiz et al., 2002, 2003), but the typical cell-division-

like structures strongly indicate a biological origin. Each of the observations *in isolation* could possibly be explained with a non-biogenic origin, but the association of a variety of these biomorphic structures, especially in one single SEM-image ($\sim 1\text{-}\mu\text{m}$ -long rods, constriction/cell-division and strings, all seen together in Fig. 10E) favours a biological origin.

We have not been able yet to determine the exact chemical–mineralogical composition of the minute and sparsely distributed structures. A relative dark appearance in the field emission SEM is indicative of low-mass elements, probably carbon. However, experimental ‘fossilisation’ of bacteria has shown that composition is a poor indicator of biogenicity, as microbes can readily become mineralised (e.g. Liebig et al., 1996; Rasmussen, 2000; Westall et al., 2000).

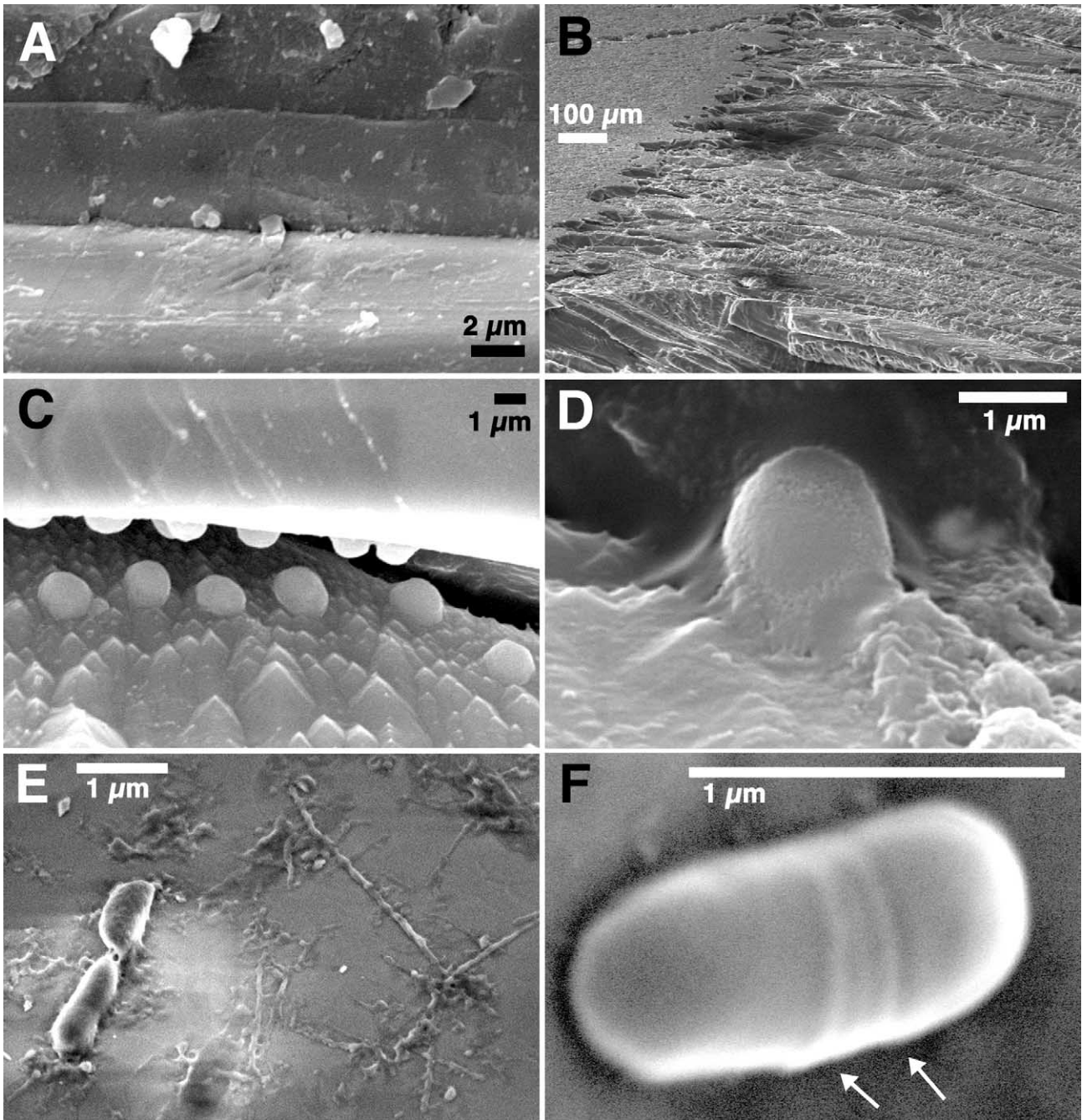


Fig. 10. Scanning electron images of biomorphic structures in calcite fibres. (A) Smooth fibre surfaces and tight horizontal fibre boundaries visible on un-etched sample. (B) Overview of etched sample, showing the rough surface created by the etching. (C) Cluster or colony of globular structures, exposed by etching of the calcite, which penetrated deeper along the fibre boundaries. Notice the similar size of all individuals. (D) Individual globular structure. (E) Linked pair of coccus-shaped structures and a network of threads. Bright 'shade' is an electric-charging effect. (F) Individual with a pair of girdles, reminiscent of wall bands that form prior to cell division. All images are gold-coated normal SEM samples, except for the uncoated sample (E), imaged with a field-emission SEM.

Excessive gold sputtering is known to produce globules that have been mistaken for small bacteria. We therefore only coated for 30 s, which avoids such unwanted artefacts (Folk and Lynch, 1997).

A final point of caution in interpreting the structures as fossil microbes is the possibility of recent contamination. The fibres are tightly packed, with fibre boundary widths well below 1 µm (Fig. 10A), and therefore too narrow for

any known archaea or bacteria to enter. The fact that the objects were only revealed by etching, and were therefore embedded *within* the calcite, excludes recent (Quaternary to laboratory) contamination of the samples by micro-organisms. The veins show no evidence whatsoever (optical, cathodoluminescence, SEM) of calcite dissolution and reprecipitation after vein formation (Elburg et al., 2002), from which we can conclude that the micro-organisms must

have lived at the time of vein growth. These would be the first fossil micro-organisms found that have such a combined age and depth: ~585 Ma and 4–6 km, respectively. The presence of micro-organisms of that age and depth is by no means controversial. Single-celled life forms have inhabited the Earth for at least over 2 Ga, and possibly up to over 3.7 Ga (Schopf, 1993; de Ronde and Ebbesen, 1996; Rosing, 1999; Shen et al., 2001; Westall et al., 2001, etc.). It is also known that life currently occurs up to several kilometres depth in the crust (Stetter et al., 1993; Liu et al., 1997; Kerr, 2002), with temperature as the limiting factor. The highest temperature at which life is known to survive is 113 °C for *Pyrolobus fumarii* (Blöchl et al., 1997). Hyperthermophile (optimum $T > 70$ °C) bacteria and archaea are currently known to survive extreme conditions, such as are found at hot springs, fumaroles, black smokers and retrieved from oil drillings (Stetter et al., 1983; Huber et al., 1989, 1990; Jones et al., 1996; Kerr, 2002). Since the veins at Oppaminda Creek formed at an estimated depth of 4–6 km, they were well within the known temperature range for hyperthermophiles to survive if the geothermal gradient was about 20 °C/km or less.

3. Discussion

The above observations indicate that calcite precipitation was mostly limited to epitaxial precipitation on existing calcite surfaces, starting with the narrow median zone veins (Figs. 7 and 8). The following observations argue against fibre growth in a (narrow) crack:

- (1) The limited growth competition is only compatible with growth on an essentially closed surface or at the most a very narrow crack (Mügge, 1928; Bons and Jessell, 1997; Hilgers et al., 2001).
- (2) Fibre growth occurred symmetrically on *both* outer surfaces. If growth were to occur in fractures, fracturing has to take place simultaneously on both sides of the vein, which is unlikely, as stress release by fracturing on one side of the vein would prevent a second parallel fracture forming on the other side. Fracturing alternating between the two sides is equally unlikely.
- (3) Smooth fibre boundaries suggest a continuous growth process, not an incremental one such as crack-sealing, which would often lead to serrated fibre boundaries (Fig. 1A). Other indications for crack-sealing, such as wall rock parallel inclusion trails, are lacking from the fibrous calcite.
- (4) The difference between the texture in the median zones and fibrous calcite indicate a distinctly different growth mechanism for the two parts of the veins. The microstructures inside the median zones bear classical indications for growth in fractures in one or multiple stages. The absence of

such microstructures in fibrous parts of veins then argues against growth into fractures.

That growth competition *can* be suppressed or even completely inhibited in a very narrow crack does not necessarily mean that fibres *do* grow in a very narrow crack as was suggested by Hilgers and Urai (2002): observations (2)–(4) still argue against a crack-seal origin. Although growth competition is suppressed in antitaxial veins, it is usually not completely absent, with a slight increase in fibre width normally visible. On an essentially closed surface, the minimum surface energy configuration would be where fibre boundaries are oriented perpendicular to the wall rock surface, here the pointed quartz crystals. This would lead to fibre boundaries to lock onto quartz crystal tips by effectively the same mechanism as proposed for growth in a narrow crack (Urai et al., 1991).

Probably the most important aspect of the veins at Oppaminda Creek (and similar veins from around the world) is the fact that they grow on both outer surfaces. Such veins do not grow by Ramsay's (1980) crack-seal mechanism. Veins that have only one growth plane at the time (stretched veins and syntaxial veins) normally do. Growth of such veins is controlled by a crack and the fluid inside that crack. Although antitaxial veins appear to be usually seeded on fracture-fill veins (the median zones), they are of a completely different nature. In a way they are more like metasomatic porphyroblasts, albeit planar and polycrystalline. Just like porphyroblasts, they grow at their outer surfaces as long as the pore fluid surrounding them is supersaturated with respect to the mineral(s) that form(s) the vein. Contrary to porphyroblasts, veins do not overgrow their host, but 'push away' the wall rock, which is possible by the 'force of crystallisation' resulting from the supersaturation of the fluid (Wiltschko and Morse, 2001). Growth will thus be fastest on vein surfaces perpendicular to the least compressive stress. There may not be a single reason for a supersaturation of the pore fluid. Although the reason for supersaturation—evaporation—in the experiments of Means and Li (2001) is completely different from whatever caused calcite supersaturation at the Oppaminda Creek veins, the resulting vein structure is very similar. For the latter veins, Elburg et al. (2002) showed that external fluids percolated through the system in which the veins grew, and suggested that these fluids may have carried excess dissolved calcite that provided the necessary supersaturation that led to antitaxial vein growth. Another possible cause for supersaturation could be the inhibition of precipitation in the limited pore space within the shale. Putnis et al. (1995) have shown that limited space can suppress precipitation, possibly leading to large supersaturations. Finally, a non-hydrostatic stress field can be a cause for the development of supersaturations on vein surfaces, depending on their orientation.

Where veins existed in suitable orientations, calcite would precipitate on them, rather than creating new veins.

Nucleation of crystals and initiation of new cracks both require threshold supersaturations and differential stress levels, respectively, which were apparently not reached during fibrous vein growth. We will now consider the relationship between supersaturation, vein growth rate, and orientation of the stress field relative to a growing vein, if vein growth is driven by a non-hydrostatic stress field. We will assume that there are no fractures between vein and wall rock and, therefore, that the stress state within the vein equals that of the wall rock.

At a grain boundary, the equilibrium chemical potential (μ) of a solid that is dissolved in a grain boundary fluid is often expressed as a function of the normal stress acting on that grain boundary (taking compression as positive):

$$\mu = \mu_0 + \Omega(\sigma_n - P_0). \quad (1)$$

Here μ_0 is some reference potential at a certain pressure (P_0) and temperature, and Ω is the molar volume of the solid (Paterson, 1973; Durney, 1976). Here we take as a reference pressure the mean stress, which is equal to the average of the principal components of the stress tensor:

$$P_0 = \frac{(\sigma_1 + \sigma_2 + \sigma_3)}{3}. \quad (2)$$

The difference ($\Delta\mu$) between average chemical potential in the rock and on a vein surface is given by:

$$\begin{aligned} \Delta\mu &= \mu_{(\text{vein surface})} - \mu_{(\text{rock})} = \mu_0 + \Omega(\sigma_n - P_0) - \mu_0 \\ &= \Omega(\sigma_n - P_0). \end{aligned} \quad (3)$$

μ is approximately proportional to the concentration in a dilute solution, and we can express the difference (ΔC) between the average equilibrium concentration in the rock and on the vein surface as a function of the normal stress acting on the vein surface:

$$\Delta C = b(\sigma_n - P_0), \quad (4)$$

where b is a proportionality constant. A non-zero ΔC will drive dissolution and precipitation if material that is equilibrated with the average rock diffuses towards or away from the vein surface that is subject to σ_n . Supersaturation at the vein surface equals $-\Delta C$ in the end-member case where diffusion is fast enough to equalise concentrations on all surfaces.

Let us now consider an isolated vein, of half width w , that is subjected to a stress field with the least compressive stress (σ_3) oriented at an angle θ to the vein surface normal, and where the intermediate principal stress component equals the mean stress ($\sigma_2 = P_0$) and lies in the plane of the vein surface. This gives:

$$\sigma_n - P_0 = \frac{1}{2}(\sigma_3 - \sigma_1)\cos(2\theta). \quad (5)$$

To link the growth rate of the vein (dw/dt) to the orientation of the stress field relative to the vein, we make

two assumptions: the supersaturation at the vein surface equals $-\Delta C$, and the precipitation rate is proportional to supersaturation, using a rate factor R :

$$\frac{dw}{dt} = -R\Delta C = \frac{-Rb}{2}(\sigma_3 - \sigma_1)\cos(2\theta). \quad (6)$$

Eq. (6) shows that the growth rate of the vein decreases when the least compressional stress rotates away from the normal to the vein surface and reduces to zero when θ reaches 45° . In other words, higher differential stresses are needed to maintain a certain vein growth rate, when θ increases.

Fig. 11A shows an intersection of two veins in which fibres curve up to about 60° . Shading represents growth stages and shows that the younger vein only formed after some growth of the older vein, while the older vein kept growing at a low angle to its surface after the younger vein had formed. The following scenario can be envisaged to explain the formation of these veins in a rotating stress field. Differential stress ($\sigma_1 - \sigma_3$) initially builds up, because no veins are available for extension by calcite precipitation on existing calcite substrates until initial tension cracks form perpendicular to the least compressional stress direction. Differential stress drops, because fibrous calcite precipitation can now proceed on the seed veins, which become median zones of growing veins. Fibres initially grow perpendicular to the median zone (Fig. 11B), but curve around as the stress field rotates (Fig. 11C). Differential stress increases again when the angle θ increases and the growth rate on the veins decreases. The veins are increasingly less suitable to accumulate strain. At some angle θ , brittle failure is reached again, and new tension cracks form, perpendicular to the current least compressional stress direction, and oblique to existing veins (Fig. 11D). Stresses drop again, as the new veins can accommodate the tension, together with the old generation of veins, as long as they are suitably oriented for some precipitation (Fig. 11E).

Whatever the mechanism and driving force for supersaturation, it was efficient enough within the shales to enable the growth of the veins to keep up with extension without fracturing. In coarser-grained carbonate-rich layers this was not the case, as microstructures within these layers indicate repeated fracturing (Fig. 9). Stresses inside the coarser layers may have been higher if these layers were mechanically more competent. Alternatively, fibrous growth may have been less efficient in these layers due to a possibly lower diffusivity and therefore less efficient nutrient transport, or some effect of the local mineralogy or chemistry that affected the growth rate or level of supersaturation. What the exact cause is for the difference between the microstructure in the fine-grained shale and the coarser carbonate layers remains unknown. However, we suggest that it may contain the clue for a future explanation of antitaxial fibrous vein growth.

An interesting, but speculative, additional cause for

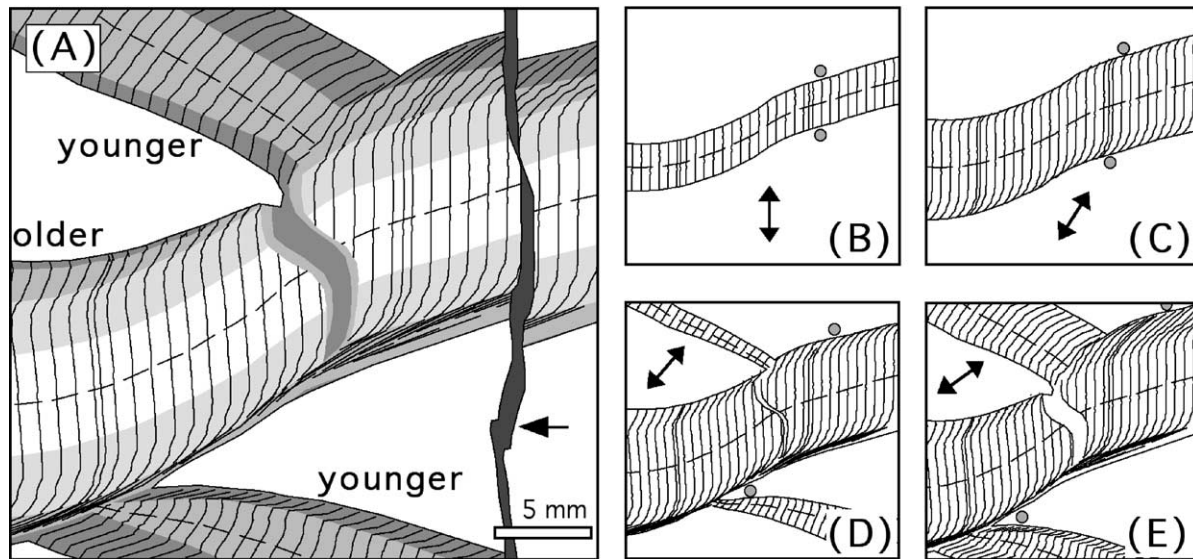


Fig. 11. (A) Drawing after a micrograph of a vein intersection from Oppaminda Creek. Shading represents growth stages from oldest (light) to youngest (dark). (B)–(E) Four stages in the development of the vein intersection. Double arrows indicate the current fibre growth direction. Two small circles represent material points and indicate the total offset across the older vein. Continued growth of the older vein, after formation of the younger vein, offset the younger vein and split the vein intersection into two T-junctions. A later non-fibrous calcite vein (arrow in (A)) cuts through and offsets the older vein.

supersaturation at the veins could be the presence of micro-organisms. The association of micro-organisms with carbonate precipitation is a common one: Folk (1999) demonstrated mineralised bacteria in many different calcite precipitates, and both Trewin and Knoll (1999) and Budai et al. (2002) reported fossil bacteria in shallow calcite veins in Devonian rocks from Great Britain and the USA, respectively. The metabolism of chemolithotrophic micro-organisms commonly leads to calcite precipitation as a by-product (Folk, 1999). Another common by-product is pyrite. The hyperthermophile *Pyrodictium*, for example, typically lives by metabolising sulphur ($4\text{H}_2 + \text{H}_2\text{S}_2\text{O}_3 \rightarrow 2\text{H}_2\text{S} + 3\text{H}_2\text{O}$) (Huber et al., 1990; see also Lodish et al., 1995; Voet and Voet, 1995), leading to precipitation of pyrite. Pyrite and chalcopryrite are minor constituents of the shale and veins at Oppaminda Creek. Elburg et al. (2002) have shown that vein formation was associated with the depletion of not only Ca and Sr from the wall rock, but also S and Cu. These observations are consistent with, but not proof for, metabolism of chemolithotroph hyperthermophiles within the veins.

The presence of fossil micro-organisms within the veins opens up some exciting new perspectives and questions. What was the role of the micro-organisms in the vein formation? Were they merely passive players, profiting from an apparently suitable environment (pore space, chemical environment)? Or were they actively involved in precipitating calcite, thereby also entombing themselves? If so, this is probably the first reported case of ‘life-assisted rock deformation’ (of course, excluding human-induced rock deformation).

Fossil micro-organisms that lived at shallow depth (sea floor) have been found back to the Archaean (see above),

but so far no Precambrian fossil life at any significant depth has been discovered. When did hyperthermophiles reach the deeper parts of the current biosphere? Did life originate in seafloor hydrothermal vents, as is commonly assumed (Schopf, 1999, 2002; Rasmussen, 2000), and then spread to deeper levels, or did it form at depth and spread to the surface? In either case, when did it happen? These questions cannot be answered here. However, the fossil micro-organisms in the veins open up one new avenue towards answering these questions. The micro-organisms found in the veins are associated with a distinct antitaxial, fibrous vein texture. If this texture is in some way related to the presence of micro-organisms, then antitaxial fibrous veins may perhaps be useful ‘fossil footprints’ of deep microbial life, which may aid us in finding more and older microfossils, and thereby giving us more insight into the origin of life on Earth.

4. Conclusions

Based on a population of antitaxial fibrous veins found at Oppaminda Creek, South Australia, we propose to redefine the term ‘antitaxial’ to apply only to those veins that have two simultaneous growth planes at the outside of a vein. With this definition, antitaxial veins can be correlated with a single growth mechanism: epitaxial overgrowth on the surface of existing veins, without the presence of fractures. Examples from Oppaminda Creek and Sestri Levante show that nucleation of the veins is by brittle fracturing, which produces the seed veins that remain as median zones in the centre of antitaxial veins. The veins at Oppaminda Creek show a consistent evolution in fibre growth direction, which

indicates that the extension direction rotated over 90° relative to the veins. A non-hydrostatic stress field can drive mineral precipitation on the vein surfaces, but other factors may play a role as well, such as, for example, influx of supersaturated fluids or even microbial metabolism.

Antitaxial veins have well developed fibres because crystallographically controlled growth competition is suppressed relative to crystal growth in cracks. The fibre width is controlled by the structure of the vein surface, which is composed of a thin rim of quartz crystals in case of the antitaxial calcite veins from Oppaminda Creek, and other examples from across the world. Antitaxial veins keep growing as long as they are suitably oriented relative to the applied stress field, even after new generations of veins have formed.

Fossil microbes were found embedded in the ~585 Ma calcite veins from Oppaminda Creek, which formed at an estimated depth of 4–6 km (not corrected for compaction of overlying sediments). We suggest that these microbes, probably hyperthermophile archaea, could have played a role in the formation of the veins, by enhancing the precipitation of calcite.

Acknowledgements

A.-J. Bons, ExxonMobil Chemical Europe Inc. is thanked for analysing samples with the field-emission SEM, and for critical discussions of the SEM observations. K.O. Stetter is greatly acknowledged for his useful help in interpreting the fossil microbes. The Sprigg family is thanked for their hospitality and access to their Arkaroola property. N.H.S. Oliver is thanked for pointing out the veins at Oppaminda Creek, and C.W. Passchier and D. Köhn for introducing the first author to the Sestri Levante veins. The Dutch Dr Schürmann Fund for Precambrian Research financed part of the fieldwork in Australia. Contributions from the other Arkaroola Research Team members, R.J. Bakker, M.A. Elburg and S. Hore, are gratefully acknowledged. R.L. Folk is thanked for his assessment of the putative microbes and D. Durney for an extremely thorough review.

References

Aerden, D.G.A.M., 1996. The pyrite-type strain fringes from Lourdes (France): indicators of Alpine thrust kinematics in the Pyrenees. *Journal of Structural Geology* 18, 75–91.

Beutner, E.C., Diegel, F.A., 1985. Determination of fold kinematics from syntectonic fibres in pressure shadows, Martinsburg Slate, New Jersey. *American Journal of Science* 285, 16–50.

Blöchl, E., Rachel, S., Burggraf, D., Hafenbradl, H., Jannasch, W., Stetter, K.O., 1997. *Pyrolobus fumarii*, gen. and sp. nov., represents a novel group of archaea, extending the upper temperature limit for life to 113 °C. *Extremophiles* 1, 14–21.

Bons, P.D., 2000. The formation of veins and their microstructures. In: Jessell, M.W., Urai, J.L. (Eds.), *Stress, Strain and Structure—A Volume in Honour of W.D. Means*. *Journal of the Virtual Explorer* 2.

Bons, P.D., 2001. Development of crystal morphology during uniaxial growth in a progressively widening vein: I. The numerical model. *Journal of Structural Geology* 23, 865–872.

Bons, P.D., Jessell, M.W., 1997. Experimental simulation of the formation of fibrous veins by localised dissolution–precipitation creep. *Mineralogical Magazine* 61, 53–63.

Brasier, M.D., Green, O.R., Jephcoat, A.P., Kleppe, A.K., Van Kranendonk, M.J., Lindsay, J.F., Steele, A., Grassineau, N.V., 2002. Questioning the evidence for Earth's oldest fossils. *Nature* 416, 76–81.

Budai, J.M., Martini, A.M., Walter, L.M., Ku, T.C.W., 2002. Fracture-fill calcite as a record of microbial methanogenesis and fluid migration: a case study from the Devonian Antrim Shale, Michigan Basin. *Geofluids* 2, 163–183.

Casey, M., Dietrich, D., Ramsay, J.G., 1983. Methods for determining deformation history for chocolate tablet boudinage with fibrous crystals. *Tectonophysics* 92, 211–239.

Coats, R.P., Blissett, A.H., 1971. Regional and economic geology of the Mount Painter Province. *Geological Survey of South Australia Bulletin* 43.

Cox, S.F., 1987. Antitaxial crack-seal vein microstructures and their relationship to displacement paths. *Journal of Structural Geology* 9, 779–788.

Cox, S.F., Etheridge, M.A., 1983. Crack-seal fibre growth mechanisms and their significance in the development of oriented layer silicate microstructures. *Tectonophysics* 92, 147–170.

Drexel, J.F., Preiss, W.V. (Eds.), 1995. *The Geology of South Australia. Volume 2: The Phanerozoic*. Geological Survey of South Australia Bulletin, 54.

Drexel, J.F., Preiss, W.V., Parker, A.J. (Eds.), 1993. *The Geology of South Australia. Volume 1: The Precambrian*. Geological Survey of South Australia Bulletin, 54.

Durney, D.W., 1976. Pressure-solution and crystallization deformation. *Philosophical Transactions of the Royal Society, London* A283, 229–240.

Durney, D.W., Ramsay, J.G., 1973. Incremental strains measured by syntectonic crystal growths, in: De Jong, K.A., Scholten, K. (Eds.), *Gravity and Tectonics*. John Wiley & Sons, New York, pp. 67–96.

Elburg, M.A., Bons, P.D., Dougherty-Page, J., Janka, C.E., Newman, N., Schaefer, B., 2001. Age and metasomatic alteration of the Mt. Neill Granite at Nooldoonooldoona Waterhole, Mt Painter Inlier, South Australia. *Australian Journal of Earth Sciences* 48, 721–730.

Elburg, M.A., Bons, P.D., Foden, J., Passchier, C.W., 2002. The origin of fibrous veins: constrains from geochemistry. *Geological Society, London, Special Publications* 200, 103–118.

Elburg, M.A., Bons, P.D., Foden, J., Brugger, J., 2003. A newly defined Late Ordovician magmatic-thermal event in the Mt Painter Province, northern Flinders Ranges, South Australia. *Australian Journal of Earth Sciences* 50, 611–631.

Elliot, D., 1972. Deformation paths in structural geology. *Bulletin of the Geological Society of America* 83, 2621–2638.

Etchecopar, A., Malavieille, J., 1987. Computer models of pressure shadows: a method for strain measurement and shear-sense determination. *Journal of Structural Geology* 9, 667–677.

Fisher, D., Brantley, S.L., 1992. Models of quartz overgrowth and vein formation: deformation and fluid flow in an ancient subduction zone. *Journal of Geophysical Research* 97, 20,043–20,061.

Foden, J., Barovich, K.M., Jane, M., O'Halloran, G., 2001. Sr-isotopic evidence for late Neoproterozoic rifting in the Adelaide geosyncline at 586 Ma: implications for a Cu ore forming fluid. *Precambrian Research* 106, 291–308.

Folk, R.L., 1999. Nannobacteria and the precipitation of carbonate in unusual environments. *Sedimentary Geology* 126, 47–55.

Folk, R.L., Lynch, F.L., 1997. The possible role of nannobacteria (dwarf

- bacteria) in clay-mineral diagenesis and the importance of careful sample preparation in high-magnification SEM study. *Journal of Sedimentary Research* 67, 583–589.
- Foxford, K.A., Nicholson, R., Polya, D.A., Hebblethwaite, R.P.B., 2000. Extensional failure and hydraulic valving at Minas da Panasqueira, Portugal: evidence from vein spatial distributions, displacements and geometries. *Journal of Structural Geology* 22, 1065–1086.
- García-Ruiz, J.M., Carnerup, A., Christy, A.G., Welham, N.J., Hyde, S.T., 2002. Morphology: an ambiguous indicator of biogenicity. *Astrobiology* 2, 353–375.
- García-Ruiz, J.M., Hyde, S.T., Carnerup, A.M., Christy, A.G., van Kranendonk, M.J., Welham, N.J., 2003. Self-assembled silica-carbonate structures and detection of ancient microfossils. *Science* 302, 1194–1197.
- Hilgers, C., Urai, J.L., 2002. Microstructural observations on natural syntectonic fibrous veins; implications for the growth process. *Tectonophysics* 352, 257–274.
- Hilgers, C., Köhn, D., Bons, P.D., Urai, J.L., 2001. Development of crystal morphology during uniaxial growth in a progressively widening vein: II. Numerical simulations of the evolution of antitaxial fibrous veins. *Journal of Structural Geology* 23, 873–885.
- Huber, R., Kurr, M., Jannasch, H.W., Stetter, K.O., 1989. A novel group of abyssal methanogenic archaeobacteria (*Methanopyrus*) growing at 110 °C. *Nature* 342, 833–834.
- Huber, R., Stoffers, P., Cheminee, J.L., Richnow, H.H., Stetter, K.O., 1990. Hyperthermophilic archaeobacteria within the crater and open-sea plume of erupting Macdonald Seamount. *Nature* 345, 179–182.
- Jones, B., Renaut, R.W., Rosen, M.R., 1996. High-temperature (>90 °C) calcite precipitation at Waikite Hot Springs, North Island, New Zealand. *Journal of the Geological Society, London* 153, 481–496.
- Kanagawa, K., 1996. Simulated pressure fringes, vorticity, and progressive deformation, in: De Paor, D.G. (Ed.), *Structural Geology and Personal Computers*. Elsevier Science, Oxford, pp. 259–283.
- Kerr, R.A., 2002. Deep life in the slow, slow lane. *Science* 296, 1056–1058.
- Koch, A.L., 1996. What size should a bacterium be? A question of scale. *Annual Review of Microbiology* 50, 317–348.
- Koehn, D., Passchier, C.W., 2000. Shear sense indicators in striped bedding-veins. *Journal of Structural Geology* 22, 1141–1151.
- Koehn, D., Aerden, D.G.A.M., Bons, P.D., Passchier, C.W., 2001. Computer experiments to investigate complex fibre patterns in natural antitaxial strain fringes. *Journal of Metamorphic Geology* 19, 217–232.
- Koehn, D., Bons, P.D., Passchier, C.W., 2003. Development of antitaxial strain fringes during non-coaxial deformation: an experimental study. *Journal of Structural Geology* 25, 263–275.
- König, H., Messner, P., Stetter, K.O., 1988. The fine structure of the fibres of *Pyrodictium occultum*. *FEMS Microbiology Letters* 49, 207–212.
- Lee, Y.-J., Wiltshchko, D.V., Grossman, E.L., Morse, J.W., Lamb, W.M., 1997. Sequential vein growth with fault displacement: an example from the Austin Chalk Formation, Texas. *Journal of Geophysical Research* 102, 22,611–22,628.
- Liebig, K., Westall, F., Schmitz, M., 1996. A study of fossil microstructures from the Eocene Messel Formation using transmission electron microscopy. *Neues Jahrbuch für Geologie und Paläontologie Monatsheft* 4, 218–231.
- Liu, S.V., Zhou, J., Zhang, C., Cole, D.R., Gajdarziska-Josifovska, M., Phelps, T.J., 1997. Thermophilic Fe(III)-reducing bacteria from the deep subsurface: the evolutionary implications. *Science* 277, 1106–1109.
- Lodish, H., Baltimore, D., Berk, A., Zipursky, S.L., Matsudaira, P., Darnell, J., 1995. *Molecular Cell Biology*. Freeman & Co, New York.
- Madigan, M.T., Martinko, J.M., Parker, J., 2000. *Biology of Microorganisms*. Prentice Hall International, Upper Saddle River, New Jersey.
- Marroni, M., 1991. Deformation history of the Mt. Gottero Unit (Internal Ligurid units, Northern Apennines). *Bollettino della Societa Geologica Italiana* 110, 727–736.
- McKay, D.S., Gibson Jr., E.K., Thomas-Keprta, K.L., Vali, H., Romanek, C.S., Clemett, S.J., Chillier, X.D.F., Maechling, C.R., Zare, R.N., 1996. Search for past life on Mars: possible relic biogenic activity in Martian meteorite ALH84001. *Science* 273, 924–930.
- McKirdy, D.M., Sumartojo, J., Tucker, D.H., Gostin, V.A., 1975. Organic, mineralogic and magnetic indications of metamorphism in the Tapley Hill Formation, Adelaide Geosyncline. *Precambrian Research* 2, 345–373.
- McLaren, S., Dunlap, W.J., Sandiford, M., McDougall, I., 2002. Thermochronology of high heat-producing crust at Mount Painter, South Australia: implications for tectonic reactivation of continental interiors. *Tectonics* 21, 1020.
- Means, W.D., Li, T., 2001. A laboratory simulation of fibrous veins: some first observations. *Journal of Structural Geology* 23, 857–863.
- Mildren, S., Sandiford, M., 1995. Heat refraction and low-pressure metamorphism in the northern Flinders Ranges, South Australia. *Australian Journal of Earth Sciences* 42, 241–247.
- Mügge, O., 1925. Über gehemmtes Kristallwachstum. *Zeitschrift für Kristallographie* 62, 415–442.
- Mügge, O., 1928. Über die Entstehung faseriger Minerale und ihrer Aggregationsformen. *Neues Jahrbuch für Mineralogie, Geologie und Paläontologie* 58A 1928, 303–348.
- Nealson, K.H., 1997. Nannobacteria: size limits and evidence. *Science* 276, 1776.
- Oliver, N.H.S., Bons, P.D., 2001. Mechanisms of fluid flow and fluid-rock interaction in fossil metamorphic-hydrothermal systems inferred from vein-wallrock patterns, geometry, and microstructure. *Geofluids* 1, 137–163.
- Pabst, A., 1931. 'Pressure-shadows' and the measurement of the orientation of minerals in rocks. *Journal of the Mineralogical Society of America* 16, 55–70.
- Passchier, C.W., Trouw, R.A.J., 1996. *Microtectonics*. Springer Verlag, Berlin.
- Passchier, C.W., Urai, J.L., 1988. Vorticity and strain analysis using Mohr diagrams. *Journal of Structural Geology* 10, 755–763.
- Paterson, M.S., 1973. Nonhydrostatic thermodynamics and its geologic applications. *Reviews of Geophysics and Space Physics* 11, 355–389.
- Paul, E., Flöttmann, T., Sandiford, M., 1999. Structural geometry and controls on basement-involved deformation in the northern Flinders Ranges, Adelaide Fold Belt, South Australia. *Australian Journal of Earth Sciences* 46, 343–354.
- Pirie, N.W., 1973. On being the right size. *Annual Review of Microbiology* 27, 119–132.
- Preiss, W.V. (Compiler), 1987. *The Adelaide Geosyncline: Late Proterozoic stratigraphy, sedimentation, palaeontology and tectonics*. Geological Survey of South Australia Bulletin 53.
- Putnis, A., Prieto, M., Fernandez-Diaz, L., 1995. Fluid supersaturation and crystallization in porous media. *Geological Magazine* 132, 1–13.
- Ramsay, J.G., 1967. *Folding and Fracturing of Rocks*. McGraw-Hill, New York.
- Ramsay, J.G., 1980. The crack-seal mechanism of rock deformation. *Nature* 284, 135–139.
- Ramsay, J.G., Huber, M.I., 1983. *The Techniques of Modern Structural Geology, 1: Strain Analysis*. Academic Press, London.
- Rasmussen, B., 2000. Filamentous microfossils in a 3235-million-year-old volcanogenic massive sulphide deposit. *Nature* 405, 676–679.
- de Ronde, C.E.J., Ebbesen, T.W., 1996. 3.2 b.y. of organic compound formation near sea-floor hot springs. *Geology* 24, 791–794.
- Rosing, M.T., 1999. ¹³C-depleted carbon microparticles in >3700-Ma sea-floor sedimentary rocks from West Greenland. *Science* 283, 674–676.
- Schopf, J.W., 1993. Microfossils of the Early Archean Apex Chert: new evidence for the antiquity of life. *Science* 260, 195–218.
- Schopf, J.W., 1999. *Cradle of Life—The Discovery of Earth's Earliest Fossils*. Princeton University Press, Princeton, New Jersey.
- Schopf, J.W. (Ed.), 2002. *Life's Origin—The Beginning of Biological Evolution*. University of California Press, Berkeley and Los Angeles.
- Shen, Y., Buick, R., Canfield, D.E., 2001. Isotopic evidence for microbial sulphate reduction in the early Archean era. *Nature* 410, 77–81.

- Spencer, S., 1991. The use of syntectonic fibres to determine strain estimates and deformation paths: an appraisal. *Tectonophysics* 194, 13–34.
- Stetter, K.O., König, H., Stackebrandt, E., 1983. *Pyrodictium* gen. nov., a new genus of submarine disc-shaped sulphur reducing Archaeobacteria growing optimally at 105 °C. *Systematic and Applied Microbiology* 4, 535–551.
- Stetter, K.O., Huber, R., Blöchl, E., Kurr, M., Eden, R.D., Fielder, M., Cash, H., Vance, I., 1993. Hyperthermophilic archaea are thriving in deep North Sea and Alaskan oil reservoirs. *Nature* 365, 743–745.
- Thomas-Keppta, K.L., McKay, D.S., Wentworth, S.J., Stevens, T.O., Taunton, A.E., Allen, C.C., Coleman, A., Gibson, E.K., Romanek, C.S., 1998. Bacterial mineralization patterns in basaltic aquifers: implications for possible life in Martian meteorite ALH84001. *Geology* 26, 1031–1034.
- Thomson, B.P., Coats, R.P., Mirams, R.C., Forbes, B.G., Dalgarno, C.R., Johnson, J.E., 1964. Precambrian rock groups of the Adelaide geosyncline. *Quarterly Geological Notes of the Geological Survey of South Australia* 9, 1–19.
- Trewin, N.H., Knoll, A.H., 1999. Preservation of Devonian chemotrophic filamentous bacteria in calcite veins. *Palaios* 14, 288–294.
- Twiss, R.J., Moores, M., 1992. *Structural Geology*. W.H. Freeman and Company, New York.
- Urai, J.L., Williams, P.F., van Roermund, H.L.M., 1991. Kinematics of crystal growth in syntectonic fibrous veins. *Journal of Structural Geology* 13, 823–836.
- Voet, D., Voet, J.G., 1995. *Biochemistry*. John Wiley & Sons, New York.
- Westall, F., 1999. The nature of fossil bacteria: a guide to the search for extraterrestrial life. *Journal of Geophysical Research* 104, 16437–16451.
- Westall, F., Steele, A., Toporski, J., Walsh, M., Allen, C., Guidry, S., McKay, D., Gibson, E., Chafetz, H., 2000. Polymeric substances and biofilms as biomarkers in terrestrial materials: implications for extraterrestrial samples. *Journal of Geophysical Research* 105, 24,511–24,527.
- Westall, F., de Wit, M.J., Dann, J., van der Gaast, S., de Ronde, C.E.J., Gerneke, D., 2001. Early Archaean fossil bacteria and biofilms in hydrothermally-influenced sediments from the Barberton greenstone belt, South Africa. *Precambrian Research* 106, 93–116.
- Williams, P.F., Urai, J.L., 1989. Curved vein fibres: an alternative explanation. *Tectonophysics* 158, 311–333.
- Wiltschko, D.V., Morse, J.W., 2001. Crystallization pressure versus “crack seal” as the mechanism for banded veins. *Geology* 29, 79–82.
- Wingate, M.T.D., Campbell, I.H., Compston, W., Gibson, G.M., 1998. Ion microprobe U–Pb ages for Neoproterozoic basaltic magmatism in south-central Australia and implications for the breakup of Rodinia. *Precambrian Research* 87, 135–159.